International Journal of Innovative Research in Advanced Engineering (IJIRAE) ISSN: 2349-2163
Volume 1 Issue 10 (November 2014) www.ijirae.com

SEISMIC STABILITY ANALYSIS OF HIGHWAY EMBANKMENT BY DIFFERENT GROUND MODIFICATION TECHNIQUES

Sabahat A. Khan*
Assistant Professor,
Civil Engg. Deptt., AMU, Aligarh, India

Syed M. Abbas
Professor,
Civil Engg. Deptt., JMI, New Delhi, India

Abstract— Seismic slope stability computations have become one of the most important activities in geotechnical earthquake engineering. The main objective of the present research was to carry out seismic slope stability analysis of a highway embankment using FEM based software (PLAXIS 2D) over a soft subsoil by using fly ash as fill material and installing geogrids to prevent settlements under highway embankments. The settlement at the crest, bottom & toe of the embankment was observed for different embankment materials. The engineering properties of the embankment materials used in numerical analysis were obtained from tests performed by various researchers. Mohr coulomb model was used for embankment material modelling and a real accelerogram of an earthquake recorded by USGS in 1989 was used for the FEM analysis. Maximum horizontal and vertical displacement and maximum acceleration caused by the earthquake in fly ash fill embankment were found to be least at the crest, bottom and toe of the embankment.

Keywords— Slope Stability, Ground Improvement Techniques, Earthquakes, Embankment, Finite Element Method

I. INTRODUCTION

Sudden ground motion during an earthquake can induce significant inertia forces in an embankment slope. These induced inertia forces change their directions alternatively with magnitude many times. Thus, the factor of safety of a slope may drop below unity several times during an earthquake. Therefore when the overall displacements exceed a certain limit, the slope may be considered to have failed. To analyze the stability of slopes under dynamic conditions several methods have been used by the researchers. Seismic slope stability computations have become one of the most important activities in geotechnical earthquake engineering.

Problems due to slope instability are very common on highway embankments and cause failure due to the soil movement which results in large settlements or sliding due to inadequate shear strength, surface cracking and thereby creating difficult driving conditions and also costly rehabilitation and maintenance for the highways all across the country. Normal fill can comprise of mix of different soils like silty sand, clayey sand or silty clay etc which are commonly found embankment material at various locations in India.

Thermal power plants account for over 70 percent of power production in India generating large volumes of fly ash. Fly ash is commonly used as a highway material in embankments and approaches. Other than fly ash polymeric materials like Geogrids made of Geosynthetics have also been used in India to prevent settlements under highway embankments. Furthermore use of fly ash with geogrids has been found to be an innovative ground improvement measure in mitigating stresses and settlements induced during earthquakes. Construction of embankments on soft soils like clay with high groundwater level is extremely challenging and often requires prior analysis. Conventional limit equilibrium and finite element are the two common methods of analysis used in geotechnical engineering for designing and predicting the mechanical behaviour of embankments. The main advantages of finite element analysis over conventional limit equilibrium method are that complete interaction of the embankment foundation can be simulated and the mode of failure need not be predetermined.

In this study our aim is to carry out stability analysis of highway embankment by FEM based PLAXIS 2D software. In order to simulate the earthquake loading on the embankment, dynamic analysis was carried out. A real accelerogram of an earthquake recorded by U.S Geological Survey (USGS) in 1989 is used for the analysis. It is contained in the standard SMC format (Strong motion CD-ROM) which can be read by PLAXIS. In dynamic analysis, comparison of displacements and acceleration response of the embankment with soil, improved with fly ash layers, reinforced with geogrid and improved both with fly ash & geogrid under dynamic loading conditions was made.

Finite Element Model

A typical embankment of 8.5 metre crest width with 2:1 side slopes has been chosen for this study. The height of the embankment is 4 metre. The soft clay layer followed by well graded sand layer is assumed to be fully saturated. The embankment is constructed on soft clay in two lifts. Height of each lift is 2 metres. The finite element model has been created and analysed using PLAXIS 8.2 Professional geotechnical analysis software. Owing to the symmetry of the problem, only one half needs to be modelled. 15 noded plain strain elements have been used for discretizing both the embankment as well as the foundation material.

In dynamic analysis of embankment, the earthquake is modelled by imposing a prescribed displacement at the bottom boundary. In contrast to the standard unit of length used in PLAXIS [m], the displacement unit in the SMC format is [cm].Therefore the input value of the horizontal prescribed displacements is set to 0.01m.The vertical component of the prescribed displacement is kept zero (u_x=0.01m and u_y=0.00m). At the far vertical boundaries, absorbent boundary conditions are applied to absorb outgoing waves. In this way the boundary conditions as described above are automatically generated (Figure 1).

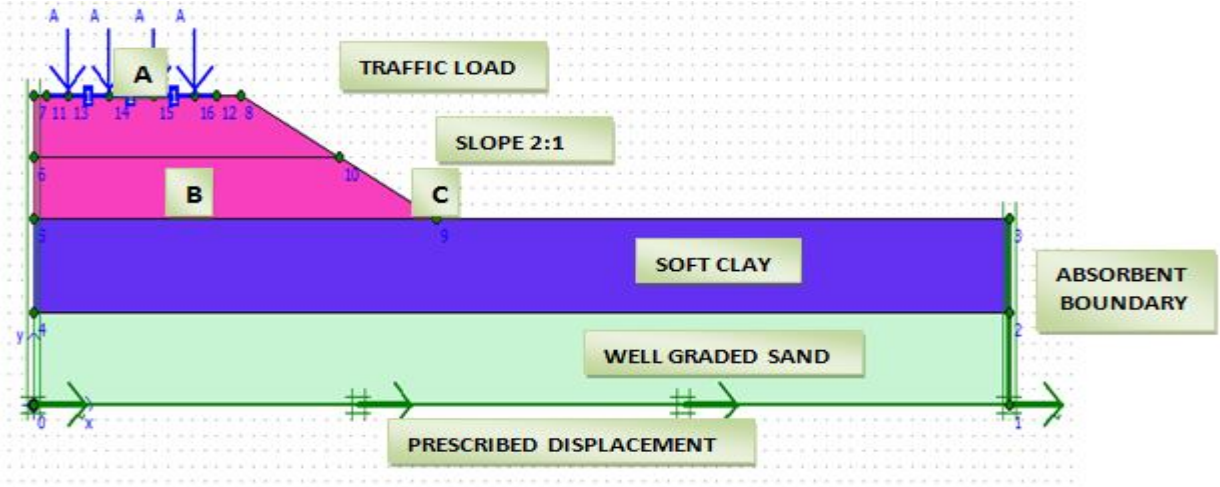

Figure 1 Geometry model with standard earthquake boundary conditions

Material Models

The embankment consisting of different materials and foundation soil comprising of soft clay and well graded sand has been modelled using the Mohr-Coulomb soil model. The embankment section also included 30 cm thick reinforced concrete pavement working platform above the existing ground. A plate element was used to simulate the pavement layer, which is placed on top of the embankment. The properties of the pavement layer are obtained from the literature and they are entered in a material set as a Young's modulus value of 30 GPa and a thickness of 0.30 m (for road). The material properties of subsoil, pavement layers and embankment materials which are used in the current modeling analysis are listed in TABLES I-IV.

TABLE I Properties of Subsoils used in FE Analysis

Subsoil Properties	**Soft Clay**	**Sand (Well-graded)**	**Unit**
Type of behaviour	Undrained	Drained	-
γ_{unsat}	15	17	kN/ m^3
γ_{sat}	18	20	kN/ m^3
k_x	1E-04	0.5	m/day
k_y	1E-04	0.5	m/day
E_{ref}	1000	30000	kN/ m^2
ν	0.33	0.3	-
c_{ref}	2	1	kN/ m^2
φ	24	34	degree
Ψ	0	4	degree
Material Model	Mohr-Coulomb (MCM)	Mohr-Coulomb (MCM)	-

TABLE II Pavement properties used in FE Analysis

Pavement Properties	**Concrete**	**Unit**
EA	1.580E+11	kN/m
EI	1.179E+09	kNm^2/m
W	1.8	kN
ν	0.15	-

TABLE III Embankment Material Properties – MCM

Embankment Properties	Normal Fill	Fly Ash	Unit
Type of behaviour	Drained	Undrained	-
γ_{unsat}	16	15.27	kN/ m^3
γ_{sat}	20	16.04	kN/ m^3
k_x	1	0.25	m/day
k_y	1	0.21	m/day
E_{ref}	3000	1747	kN/ m^2
v	0.30	0.33	-
c_{ref}	1	32	kN/ m^2
ϕ	30	31.62	degree
ψ	0	1.62	degree
Material Model	Mohr-Coulomb (MCM)	Mohr-Coulomb (MCM)	-

TABLE IV Material properties of the Geogrid

Parameter	Name	Geogrid	Unit
Material Model	Model	Elastic	-
Normal Stiffness	EA	50	kN/m

Mesh Generation

For the mesh generation, the global coarseness is set to 'medium' and the mesh is generated as shown in Figure 2.

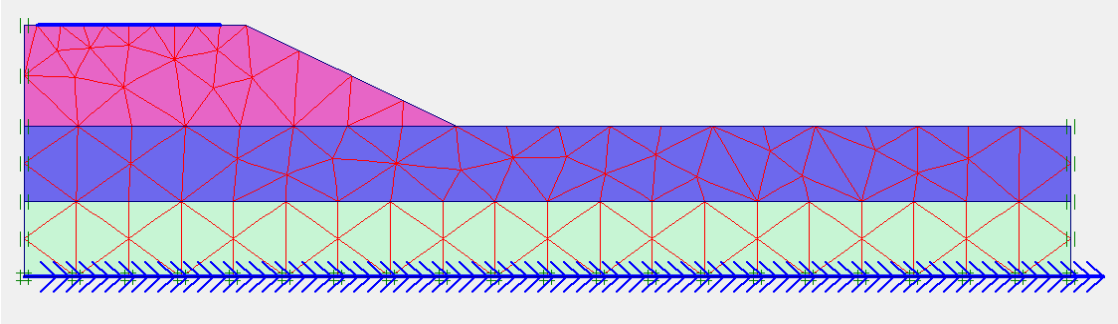

Figure 2 Finite element mesh

Initial Conditions

In the initial conditions, water unit weight was set to 10 kN/m^3. The water pressure is fully hydrostatic and is based on a general phreatic level. After the generation of water pressures, initial stresses were generated. In the initial situation the embankment as well as the pavement which is simulated by plate is present when the earthquake occurs. In the order to generate the initial stresses, the plate was activated first. After the generation of the initial stresses the input is complete and the calculations can be defined.

Calculations

The calculation involved two phases. The first one is normal plastic calculation in which the embankment is constructed. The second is a dynamic analysis in which the earthquake is simulated. To analyse the effects of the earthquake in detail the displacements are reset to zero at the beginning of each phase. Figure 3 presents a snapshot of different phases of the construction process as implemented in FEM program.

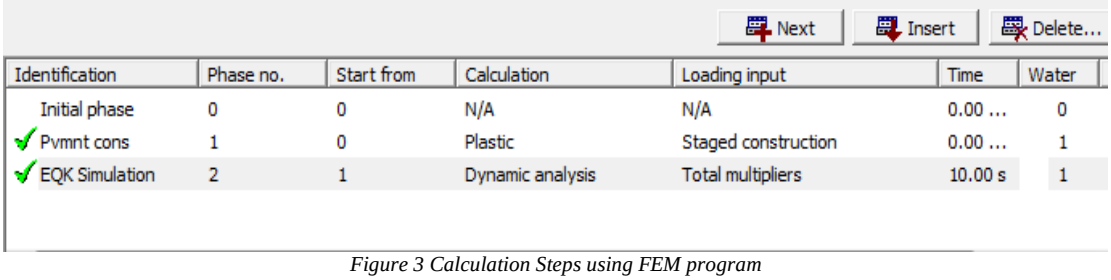

Figure 3 Calculation Steps using FEM program

Figure 4 shows an in built accelerogram which is used to simulate earthquake in the dynamic analysis in the calculation program. Duration of the earthquake was considered to be 10 s.

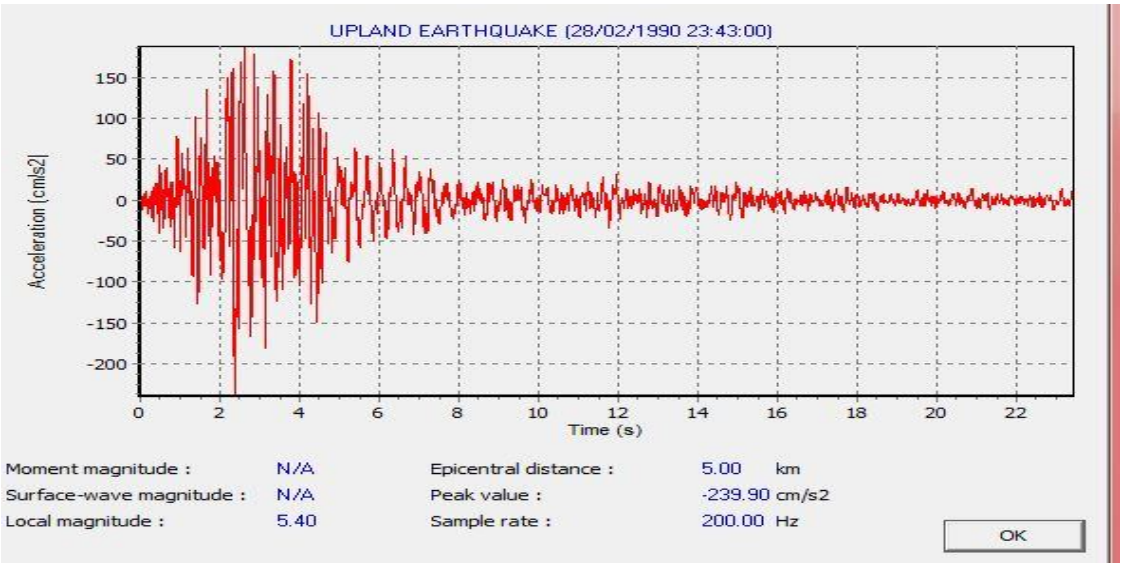

Figure 4 Accelerogram used in dynamic analysis

II. RESULTS AND DISCUSSIONS

Normal Fill Embankment

The maximum horizontal and maximum vertical displacement (or settlement) at the top of the embankment is 13 mm at t=2.8 s and 44 mm at t=4.76 s respectively. Figure 5 shows the deformed mesh showing extreme total displacement of 73.73 mm. Figure 6 and Figure 7 show, respectively, time- displacement curves and time-acceleration curves at the crest (A), bottom (B) and toe (C) of the embankment.

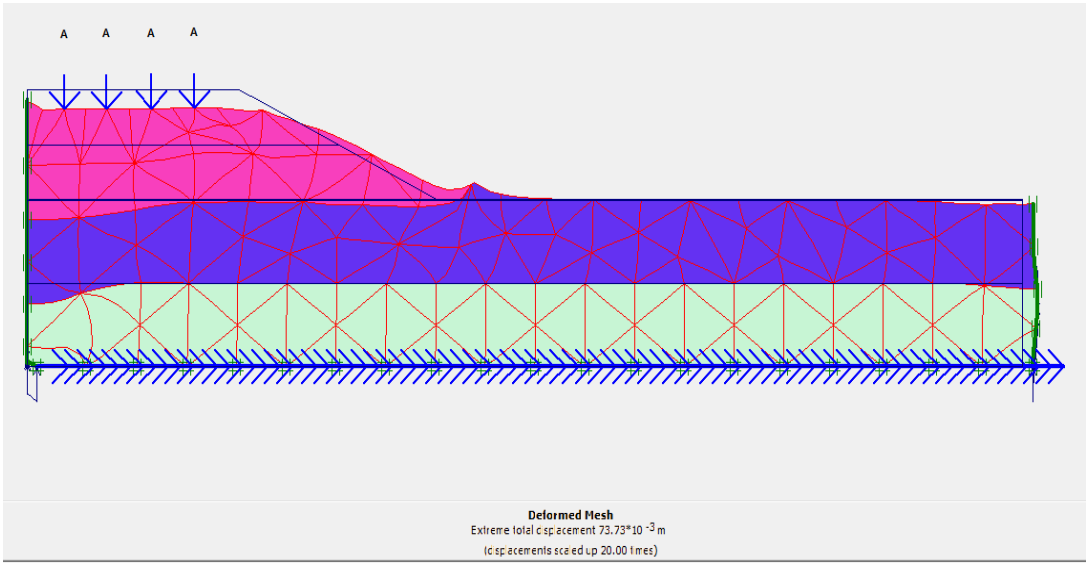

Figure 5 Deformed Mesh of Normal Fill Embankment

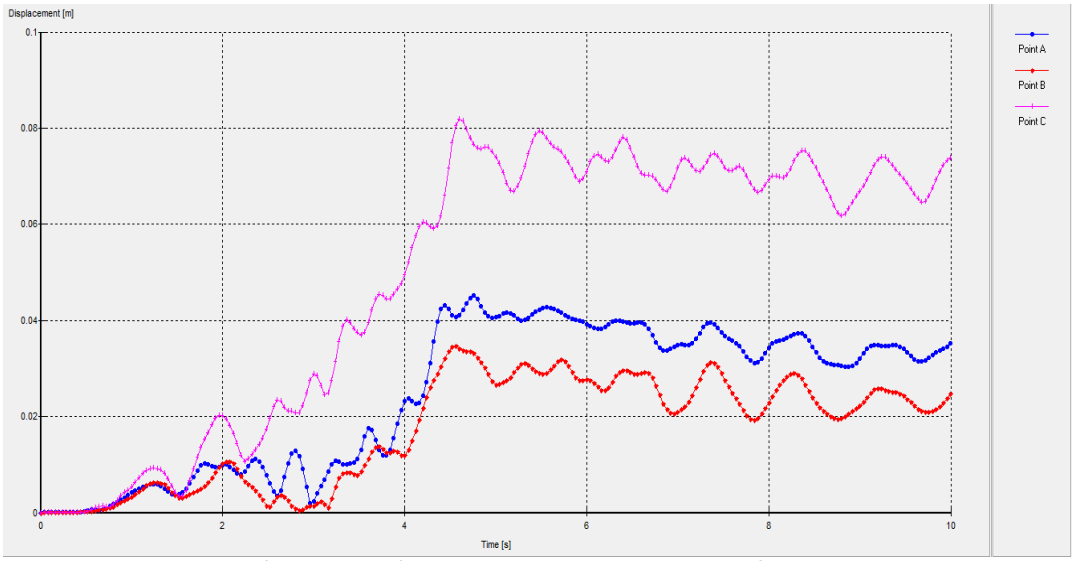

Figure 6 Time-displacement curve for the crest of the embankment (Point A), bottom of the embankment (Point B) and toe of the embankment (Point C)

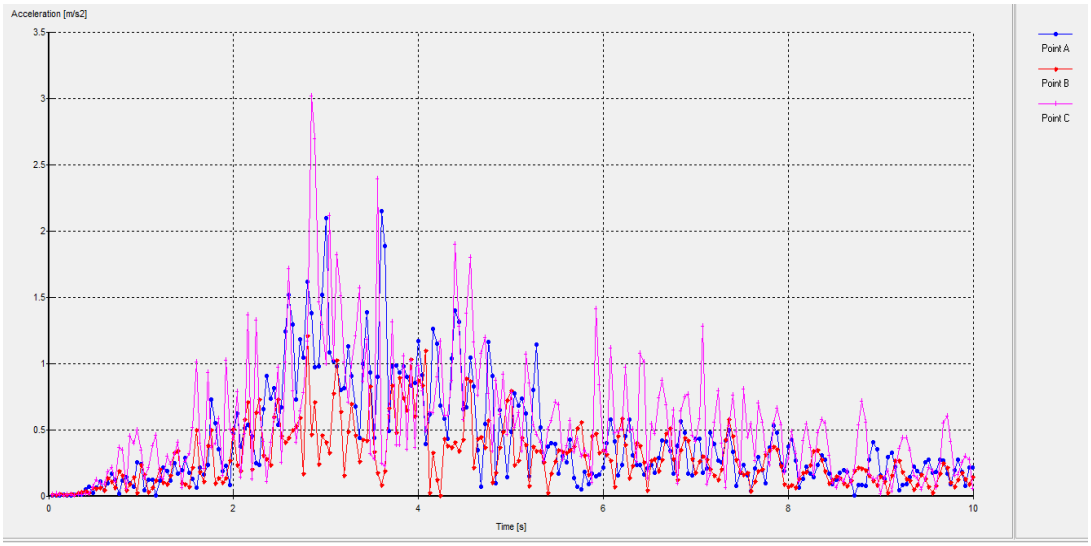

Figure 7 Time-acceleration curve for the crest of the embankment (Point A), bottom of the embankment (Point B) and toe of the embankment (Point C)

Fly Ash Fill Embankment

The maximum horizontal and maximum vertical displacement (or settlement) at the top of the embankment is 0.14 mm at t=3.44 s and 0.089 mm at t=0.6 s respectively. Figure 8 shows the deformed mesh showing extreme total displacement of 0.308 mm. Figure 9 and Figure 10 show, respectively, time-displacement curves and time-acceleration curves at the crest, bottom and toe of the embankment.

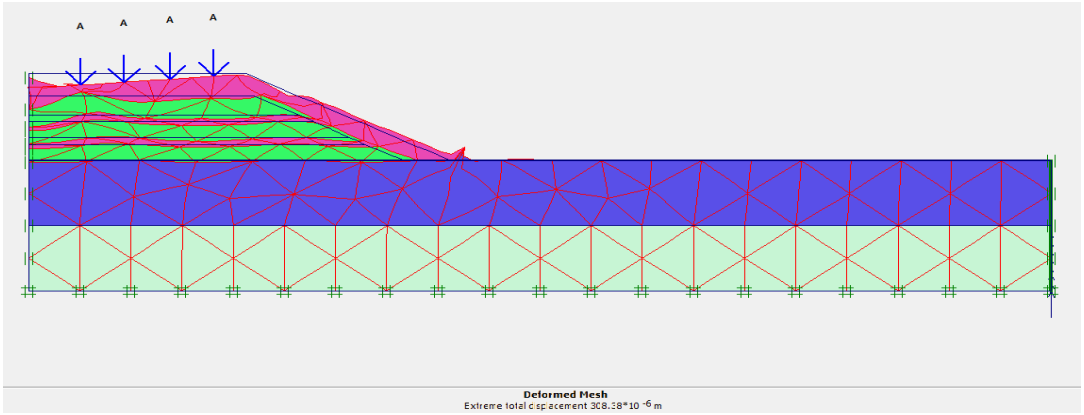

Figure 8 Deformed Mesh of Fly Ash Embankment

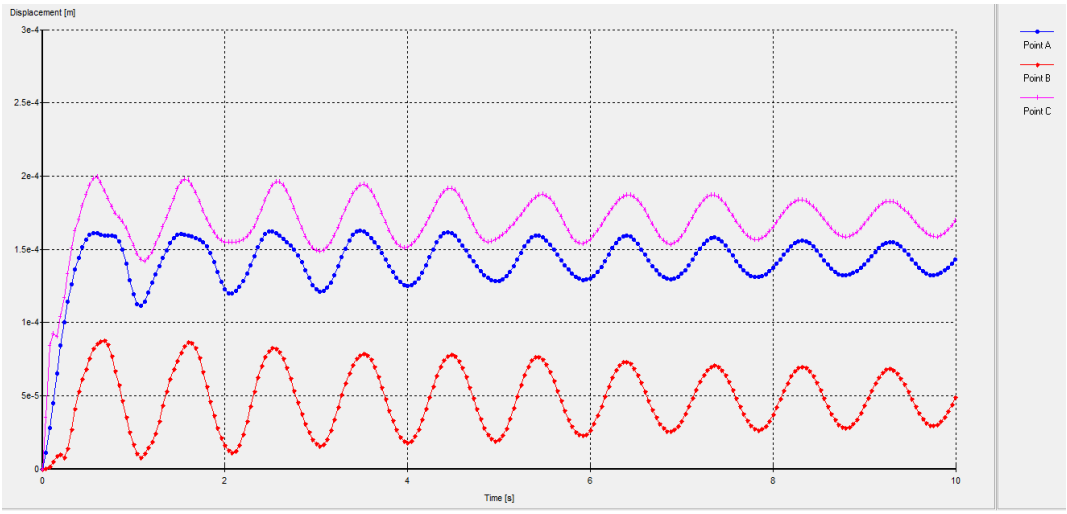

Figure 9 Time-displacement curve for the crest of the embankment (Point A), bottom of the embankment (Point B) and toe of the embankment (Point C)

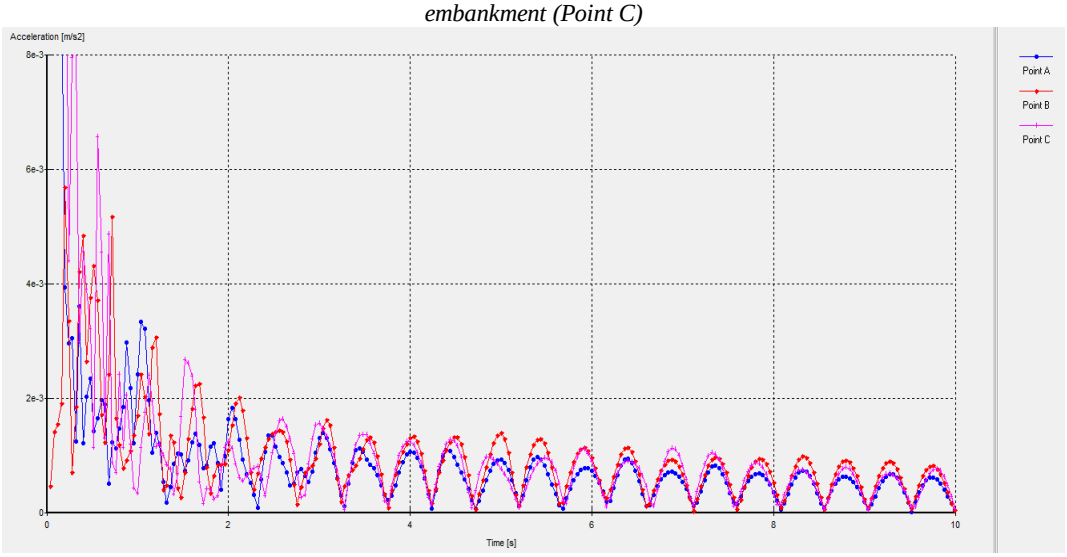

Figure 10 Time-acceleration curve for the crest of the embankment (Point A), bottom of the embankment (Point B) and toe of the embankment (Point C)

Geogrid Reinforced Normal Fill Embankment

The maximum horizontal and maximum vertical displacement (or settlement) at the top of the embankment is 12 mm at t=2.84 s and 45 mm at t=4.8 s respectively. Figure 11 shows the deformed mesh showing extreme total displacement of 109.36 mm. Figure 12 and Figure 13 show, respectively, time-displacement curves and time-acceleration curves at the crest, bottom and toe of the embankment.

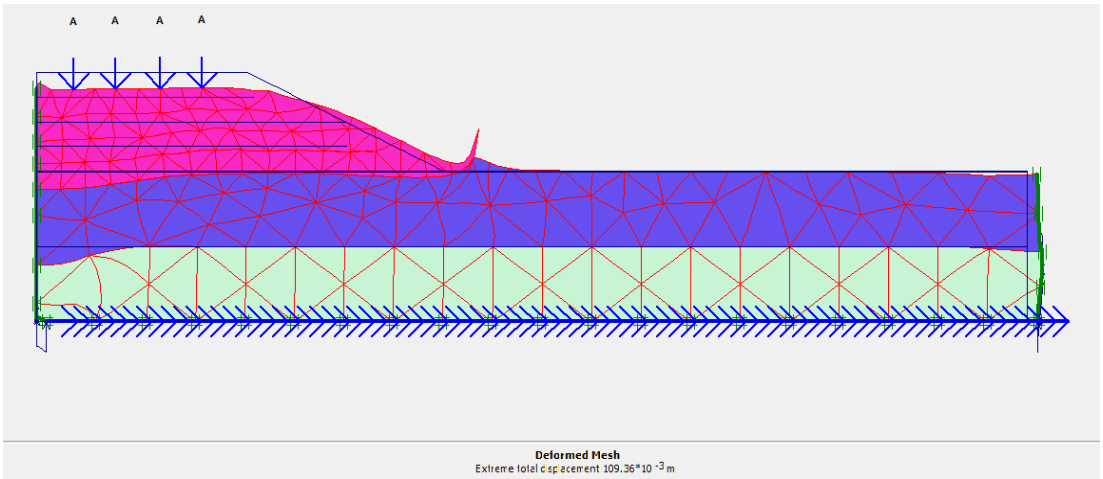

Figure 11 Deformed Mesh of Geogrid Reinforced Embankment

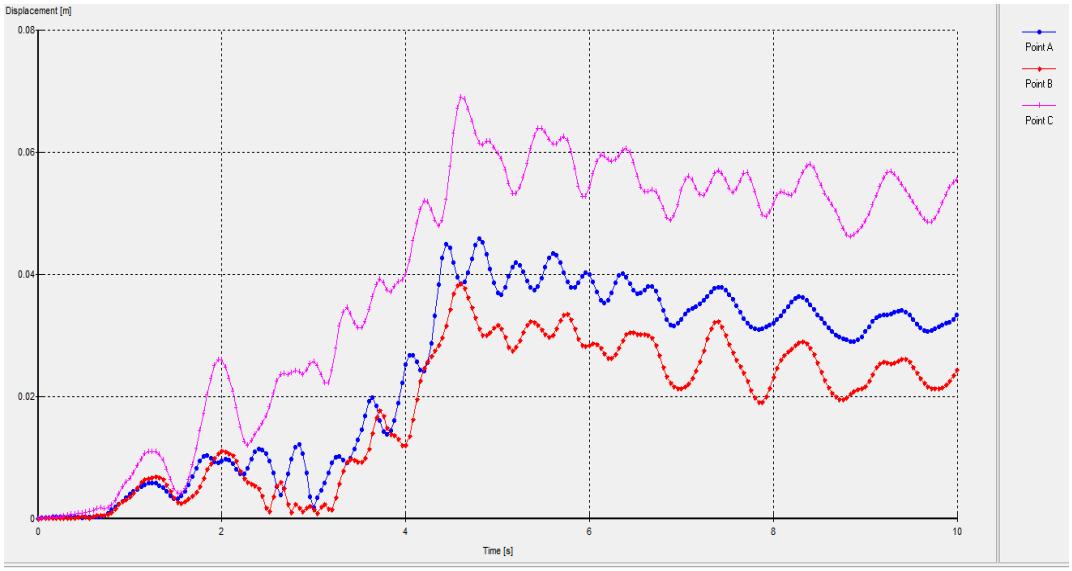

Figure 12 Time-displacement curve for the crest of the embankment (Point A), bottom of the embankment (Point B) and toe of the embankment (Point C)

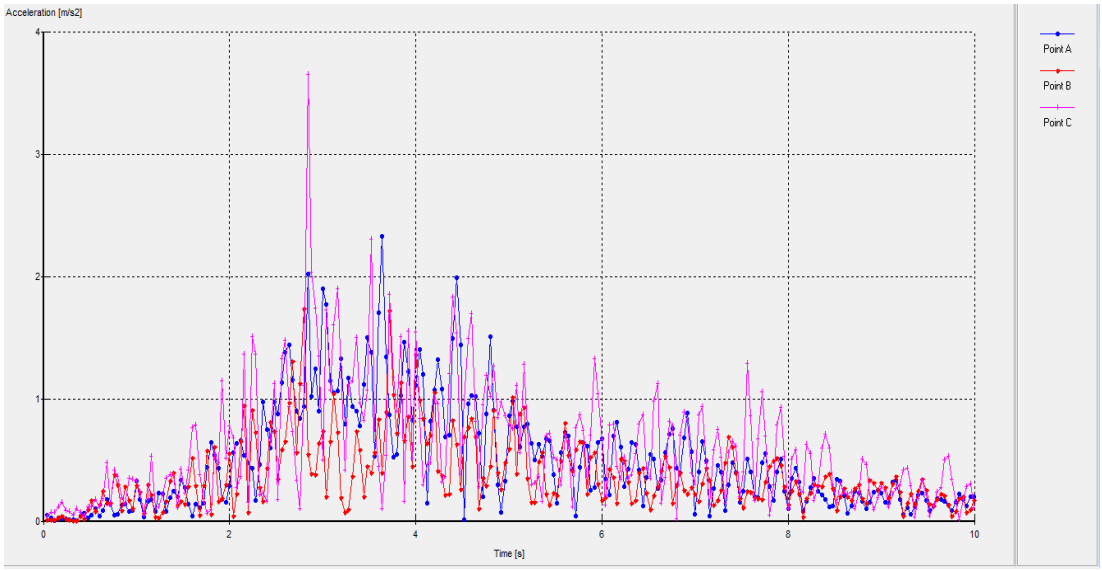

Figure 13 Time-acceleration curve for the crest of the embankment (Point A), bottom of the embankment (Point B) and toe of the embankment (Point C)

Geogrid Reinforced Fly Ash Fill Embankment

The maximum horizontal and maximum vertical displacement (or settlement) at the top of the embankment is 10 mm at t=3.52 s and 37 mm at t=4.64 s respectively. Figure 14 shows the deformed mesh showing extreme total displacement of 80.54 mm. Figure 15 and Figure 16 show, respectively, time-displacement curves and time-acceleration curves at the crest, bottom and toe of the embankment.

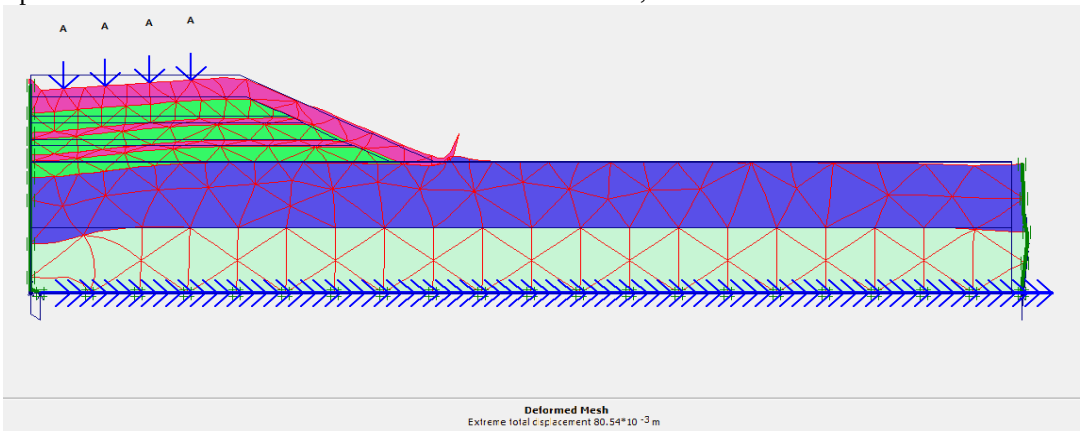

Figure 14 Deformed Mesh of Geogrid Reinforced Fly Ash Embankment

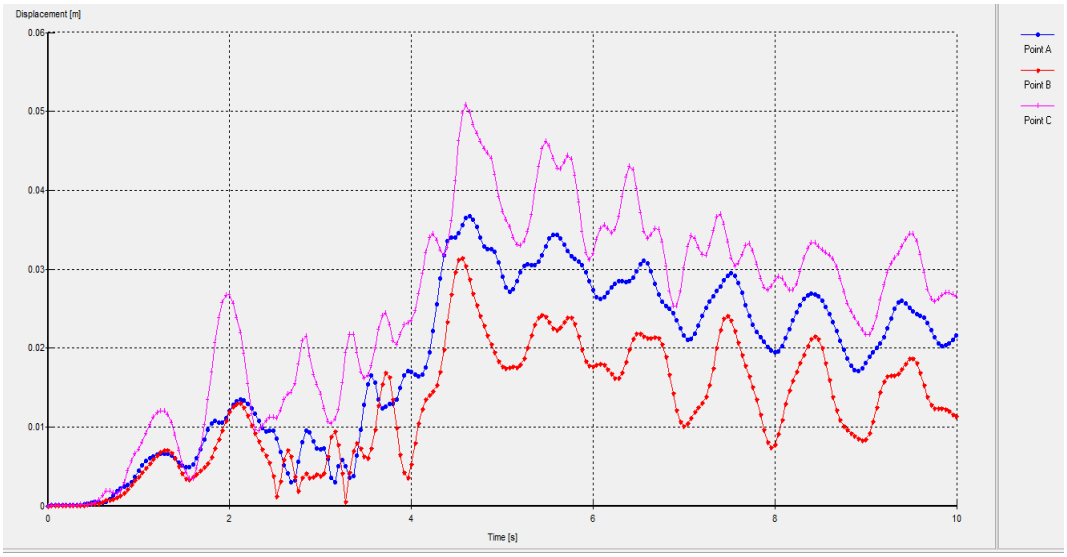

Figure 15 Time-displacement curve for the crest of the embankment (Point A), bottom of the embankment (Point B) and toe of the embankment (Point C)

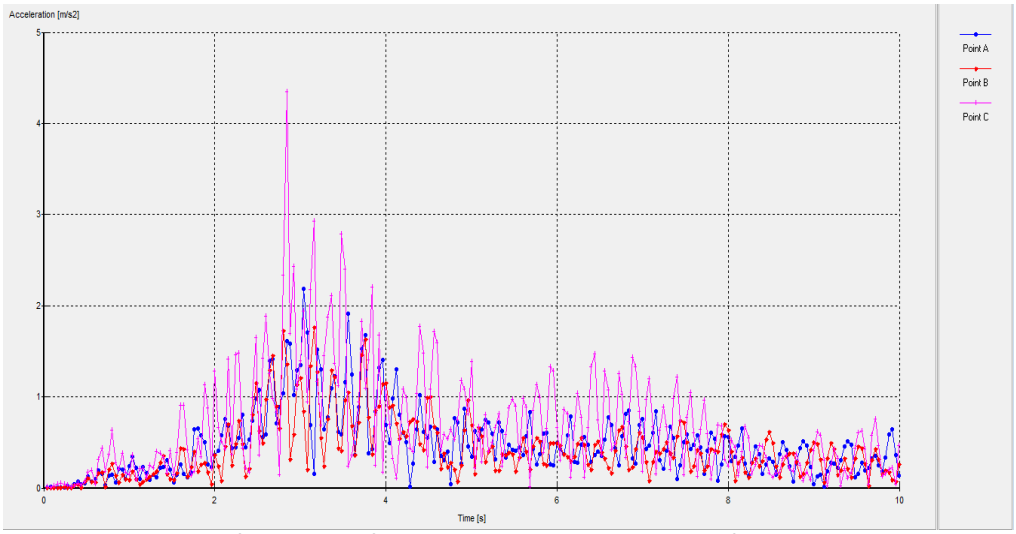

Figure 16 Time-acceleration curve for the crest of the embankment (Point A), bottom of the embankment (Point B) and toe of the embankment (Point C)

From the above figures, it can be seen that fly ash fill embankment performs better amongst the four embankment materials. Figures 17-22, below shows the variation of maximum horizontal & vertical displacement and maximum acceleration at points A, B & C for different embankment fill materials where A, B & C corresponds to the crest, bottom and toe of the embankment respectively.

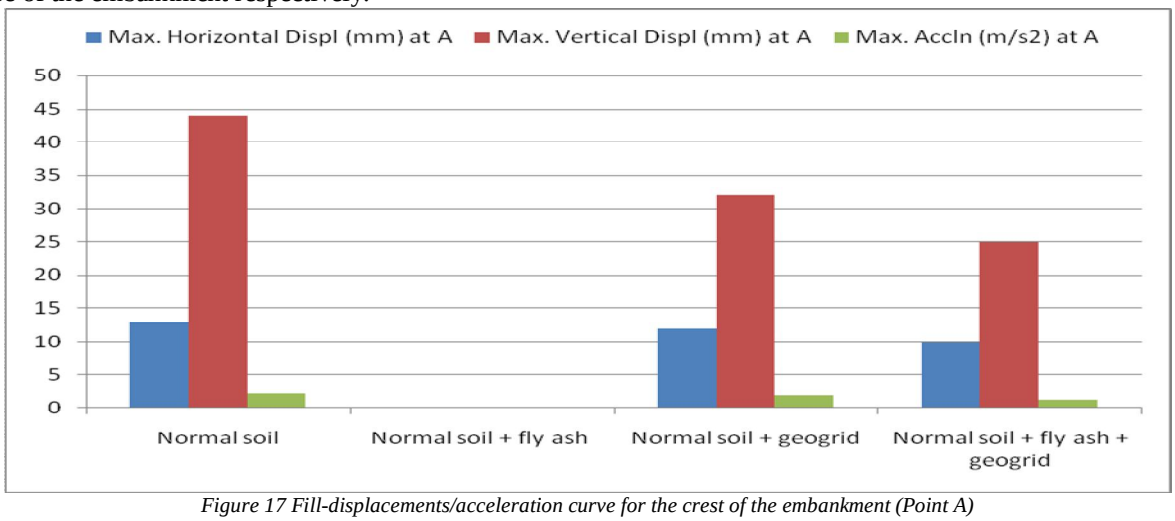

Figure 17 Fill-displacements/acceleration curve for the crest of the embankment (Point A)

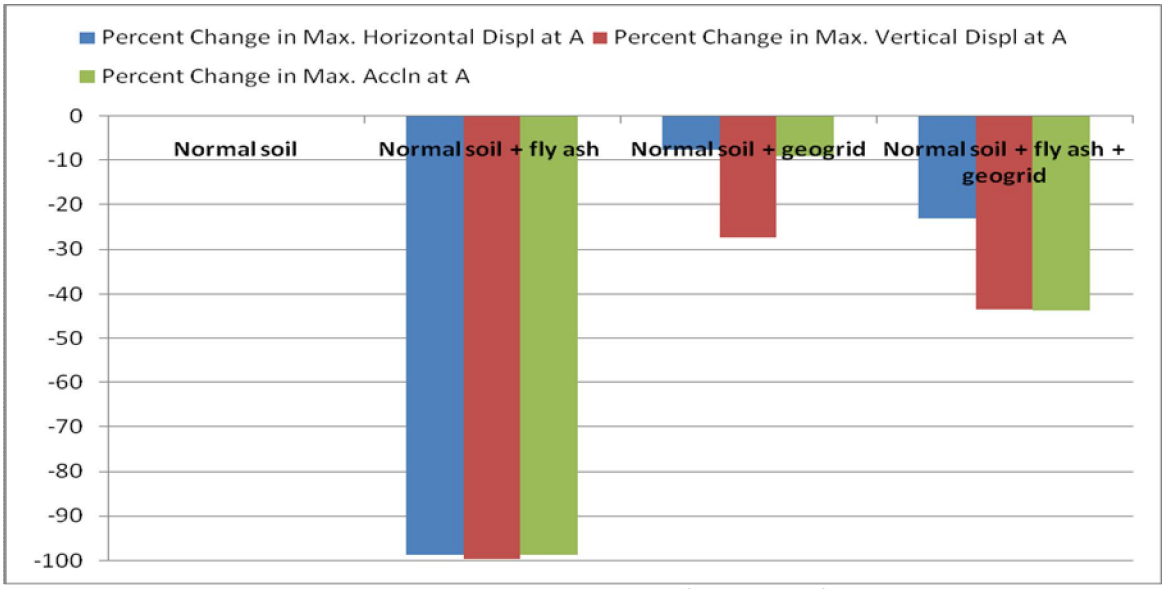

Figure 18 Fill-% change in displacements/acceleration curve for the crest of the embankment (Point A)

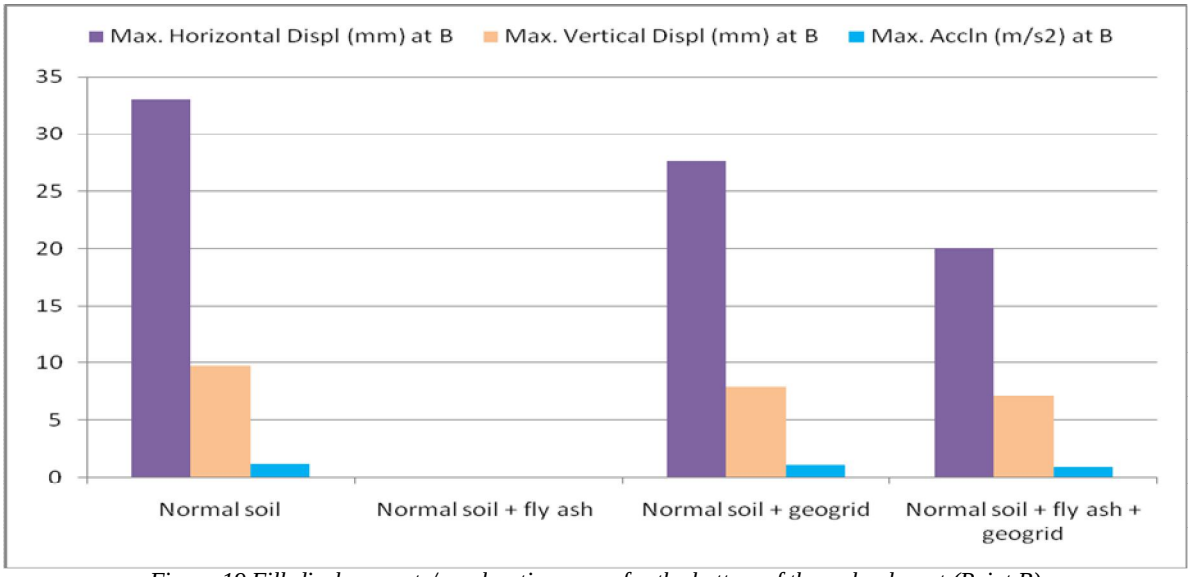

Figure 19 Fill-displacements/acceleration curve for the bottom of the embankment (Point B)

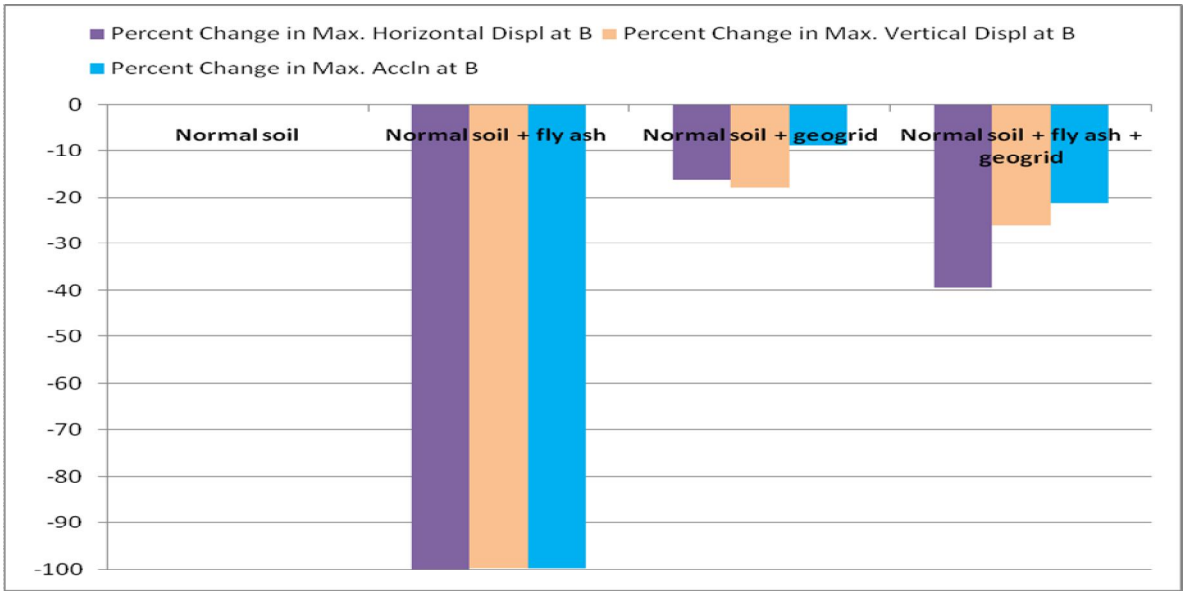

Figure 20 Fill-% change in displacements/acceleration curve for the bottom of the embankment (Point B)

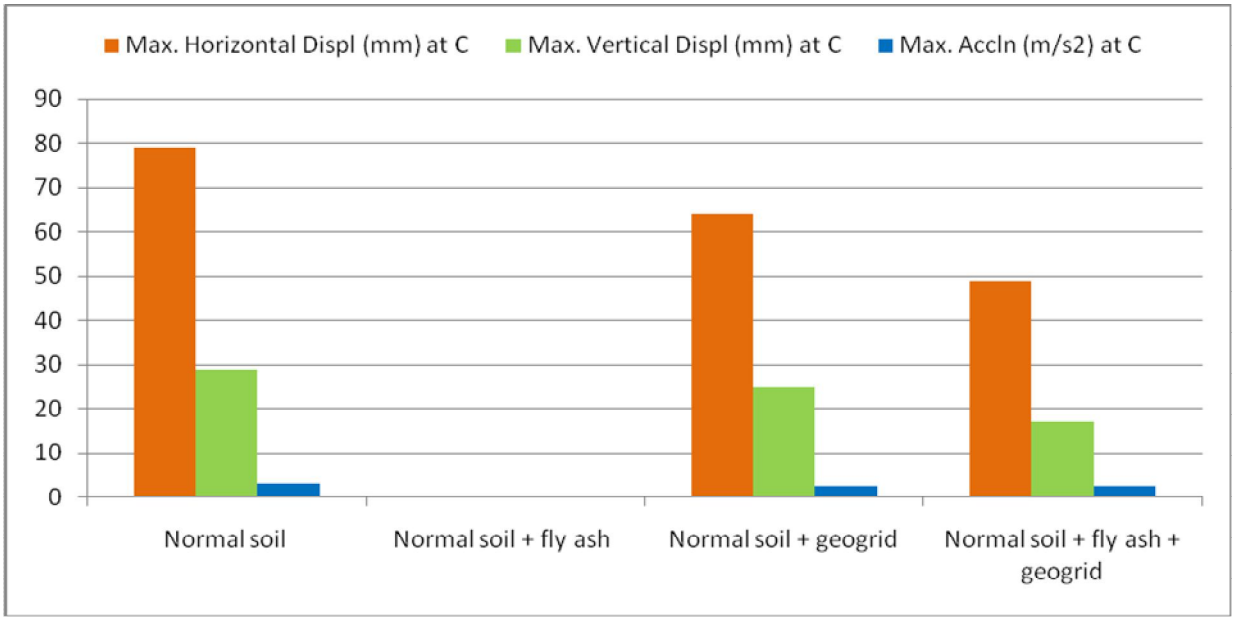

Figure 21 Fill-displacements/acceleration curve for the toe of the embankment (Point C)

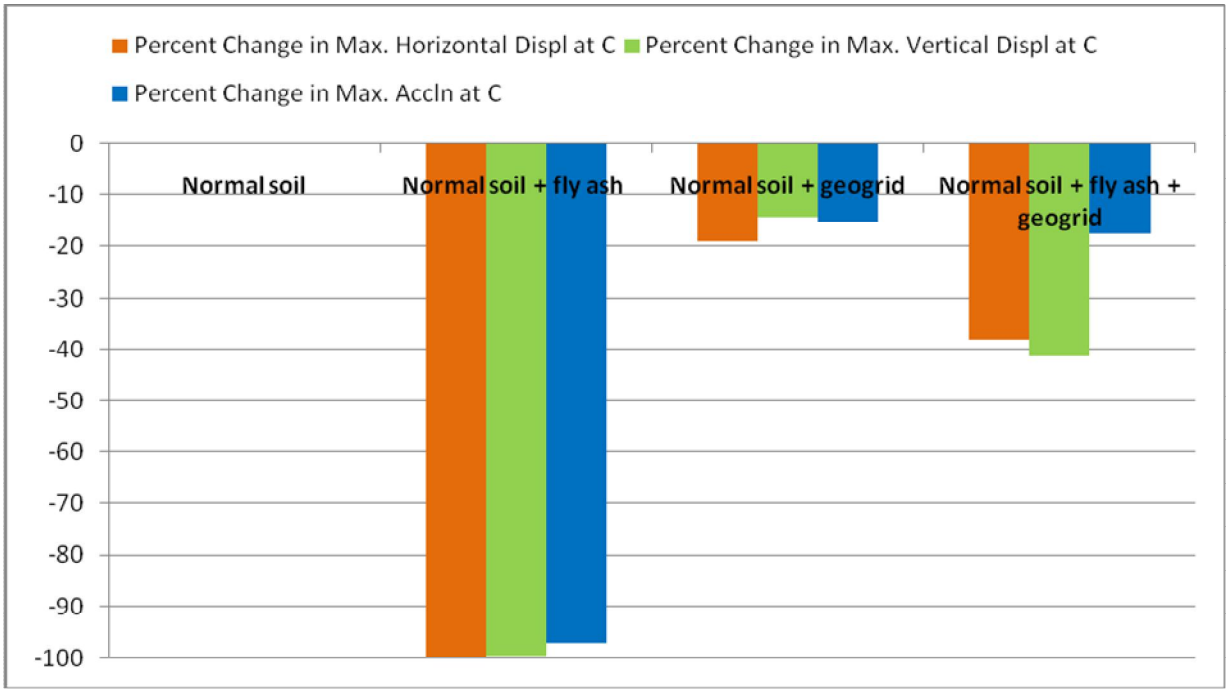

Figure 22 Fill-% change in displacements/acceleration curve for the toe of the embankment (Point C)

From the dynamic analysis of different embankment materials, it was observed that fly ash fill embankment performed well in seismic conditions. A key benefit of fly ash is its high resistance to earthquake effects (the low unit weight results in lower seismic inertial forces).

In addition to fly ash fill, other fill materials compared to normal fill embankment also showed improved performance such as fly ash reinforced with geogrid embankment due to its additional strength properties.

III. CONCLUSIONS

Maximum horizontal and vertical displacement at points A, B & C were found to be minimum in case of normal soil with fly ash layers fill embankment under earthquake loading due to reduction in unit weight of soil by addition of fly ash which subsequently resulted in low seismic inertial forces.

The maximum acceleration produced by the earthquake produced least acceleration in case of fly ash fill embankment at the crest, bottom and toe of the embankment.

REFERENCES

[1] B.M. Das, Principles of Soil Dynamics, PWS Kent, 1992, USA.
[2] Carolina Sigarán-Loría et al, Soil stability under earthquakes: A Sensitivity Analysis, 4th International conference on Geotechnical Earthquake Engineering, June 25-28, 2007, Paper No. 1763, Thessaloniki-GREECE.
[3] Emilliani Anak Geliga and Dygku Salma Awg Ismail, Geotechnical Properties of Fly Ash and its Application on Soft Soil Stabilization, Vol. 1: issue 2 /April 2010, UNIMAS E-Journal of Civil Engineering,.
[4] Ennio M. Palmeira et al, Advances in Geosynthetics Materials and Applications for Soil Reinforcement and Environmental Protection Works, 2008, EJGE.
[5] Fabio Santos et al, Geotechnical properties of Fly Ash and Soil mixtures for use in highway embankments, World of Coal Ash (WOCA) Conference, May 9-12, 2011, Denver, CO, USA.
[6] George A. Munfakh and Duncan C. Wyllie, 2000, Ground improvement engineering- Issues and selection.
[7] IRC: 36-1970, Recommended practice for the construction of earth embankments for road works.
[8] J. Koseki, Use of Geosynthetics to Improve Seismic Performance of Earth Structures, Institute of Industrial Science, the University of Tokyo, 2011, Japan.
[9] K. Banyopadhyay, S. Bhattacharjee and S. Ghosh, Numerical Approach for analysis of highway fly ash embankment, Proceedings of Indian Geotechnical Conference December 15-17, 2011, Kochi, Paper No. N-277.
[10] Kazuhiro Oda et al, Improvement Technique of Earthquake Resistance of Road Embankment through Numerical Analyses, The 14th World Conference on Earthquake Engineering, October 12-17, 2008, Beijing, China.
[11] Ken-ichi Tokida, Seismic potential improvement of road embankment, Advances in Geotechnical Earthquake Engineering – Soil Liquefaction and Seismic Safety of Dams and Monuments, Osaka University, 2012, Japan.
[12] K.V. Priyanka et al, A numerical study on the stability of slopes under seismic conditions, International Journal of Earth Sciences and Engineering 75 ISSN 0974-5904, Volume 04, No 06 SPL, October 2011, pp. 75-78.
[13] M. R. Hausmann, Engineering Principles of Ground Modifications, McGH Sydney, 1990, Australia.
[14] M. Terashi and I. Juran, 2000, Ground Improvement-State of the art.
[15] PLAXIS 8.2, Material Model Manual.
[16] Robinson, R., & Thagesen, Road Engineering for Development, 2006, CPI New York, USA.
[17] V. R. Raju, Ground Improvement- Applications and Quality Control, Indian Geotechnical Conference, GEOtrendz, December 16–18, 2010, IGS Mumbai Chapter & IIT Bombay.
[18] S. Bhuvneshwari, R. J. Robinson and S. R. Gandhi, Stabilization of expansive soils using fly ash, Fly Ash India, 2005, New Delhi.
[19] T. Tanchaisawat et al, Numerical simulation of geogrid reinforced lightweight Geomaterials on soft ground area, Proceeding of the 4th Asian Regional Conference on Geosynthetics, June 17 - 20, 2008, Shanghai, China.

